Tunable-chirp pulse compression in quasi-phase-matched second-harmonic generation

A. M. Schober, G. Imeshev, and M. M. Fejer

E. L. Ginzton Laboratory, Stanford University, Stanford, California 94305

Received December 12, 2001

We demonstrate continuously tunable compensation of linear chirp on a first-harmonic pump pulse to produce a near-transform-limited second-harmonic output pulse through the use of a chirped, fanned, periodically poled lithium niobate quasi-phase-matching grating. Compensation of positive and negative chirps is possible through reversal of device orientation. The device is simple and monolithic and can be applied to compensation of a higher-order phase with minor modification. © 2002 Optical Society of America

OCIS codes: 140.7090, 190.7110, 190.2620, 190.4360, 230.4320, 320.5520.

Shaping of the temporal profiles of optical pulses is an important tool for ultrafast optics. Recently it was demonstrated that linearly chirped gratings in quasi-phase-matched (QPM) nonlinear media can compensate for the quadratic[1–3] and higher-order[4,5] phases of chirped optical pulses during second-harmonic generation (SHG). More generally, a theory has demonstrated the potential for nearly arbitrary engineering of amplitudes and phases of short optical pulses with appropriate variation of the periods and duty cycles of aperiodic QPM gratings during SHG[6] and difference-frequency generation.[7]

Experiments have shown that QPM devices have the advantage of compact monolithic design with no critical alignment necessary but have the disadvantage of a fixed set of grating parameters with no continuous adjustability. Previously it was demonstrated that fanned gratings provide continuous tuning of the QPM period in a periodically poled lithium niobate (PPLN) optical parametric oscillator.[8] We demonstrate use of a fanned QPM grating to achieve continuous tunability of grating chirp during QPM SHG pulse compression, specifically, the compression of 140-fs-long 1.554-μm pulses stretched to 8 ps long to near-transform-limited 140-fs pulses at 777 nm. We use a chirped PPLN QPM grating with grating chirp tunable from 0.36 to 0.21 mm^{-2} that is capable of compensating for first-harmonic (FH) pulse chirps from -0.271 to -0.464 ps^2. We demonstrate pulse compression at a ratio [FH pulse width to second-harmonic (SH) pulse width] of 63 and the capability to achieve ratios of 50 to 90 with our single tunable device.

Whereas the use of a fanned grating is directly applicable to tuning more-complicated grating structures and in other second-order nonlinear interactions such as difference-frequency generation, we restrict our discussion to pulse compression in a QPM SHG experiment. The theory for QPM SHG pulse compression was described in detail in Ref. 6; here we summarize pertinent results of that research.

Effective group-velocity dispersion in a QPM pulse shaping device is the result of the interplay between the mismatch in group velocities of the FH and SH fields and the ability to spatially localize the conversion of different frequency components at different locations in the QPM device. In general, for a chirped QPM grating the maximum achievable group delay, $\tau_g = \delta\nu L$ [where $\delta\nu$ is the group-velocity mismatch parameter [$\delta\nu = ({v_{g1}}^{-1} - {v_{g2}}^{-1})$], v_{g1} and v_{g2} are the group velocities of the FH and SH fields, respectively; and L is the QPM crystal length], determines the longest chirped pulse that can be compressed with a given device. For a 5-cm-long PPLN grating designed for QPM SHG at a wavelength of 1.55 mm ($\delta\nu = 0.31$ ps/mm) the maximum group delay is 15 ps.

The local grating k-vector for a linearly chirped QPM device is

$$K_g(x) = K_m + 2D_g x\,, \tag{1}$$

where K_m is set by the phase-matching condition $K_m = \Delta k_0$ and $\Delta k_0 = 2k_1 - k_2$ is the carrier k-vector mismatch, D_g is the grating chirp parameter, and the local QPM period is $\Lambda(x) = 2\pi/K_g(x)$. A properly designed QPM SHG pulse-compression device has a SHG bandwidth of $\Delta\Omega_g = |2D_g L/\delta\nu|$ chosen to be roughly three times the FH bandwidth to reduce the effects of bandwidth truncation.[6]

Consider a chirped FH pulse with chirp parameter $C_1 = \mathrm{d}^2\Phi_1/\mathrm{d}\omega^2$ evaluated at FH carrier frequency ω_1, where Φ_1 is the FH frequency-domain phase function. The effect of the chirped QPM grating on SHG results in the following chirp on the SH pulse (defined in similar fashion to C_1 and evaluated at SH carrier frequency ω_2):

$$C_2 = 1/2(C_1 + \delta\nu^2/D_g)\,. \tag{2}$$

The result is zero SH chirp when the chirp of the QPM grating is matched to the chirp of the FH field: $D_g = -\delta\nu^2/C_1$, indicating a transform-limited SH pulse and complete pulse compression. For a more thorough discussion of QPM SHG pulse compression, see Ref. 6.

A schematic of the fanned chirped grating design is shown in Fig. 1. At one edge of the sample the grating k-vector is patterned with chirp D_a, and at the other edge the chirp is D_b. The domains are simply connected from one side of the device to the other, so the grating chirp as a function of lateral position y is the weighted average of the two defined chirps:

0146-9592/02/131129-03$15.00/0

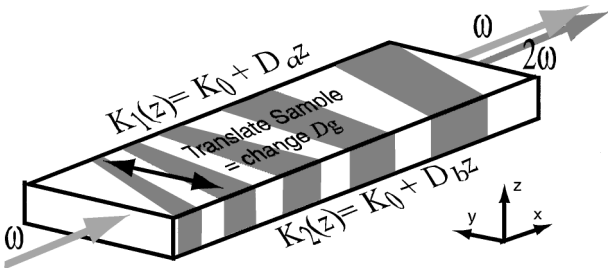

Fig. 1. Fanned QPM SHG pulse-compression grating. Translation of the sample transverse to the direction of propagation produces continuous tuning of the grating chirp. Coordinate axes are drawn to coincide with crystallographic axes in our PPLN device; reversed domains are shaded gray.

$$D_g(y) = \left(\frac{1}{2} - \frac{y}{W}\right)D_a + \left(\frac{1}{2} + \frac{y}{W}\right)D_b\,, \tag{3}$$

where W is the sample width and y is defined as zero in the center of the sample. In this manner, translation of the sample offers continuous tuning of D_g from D_a to D_b. Note that propagation through the sample in the reverse direction reverses the sign of the grating chirp, permitting continuous tuning from $-D_a$ to $-D_b$ as well, with the same device.

Whereas the grating chirp at the ends of the sample ($y = \pm W/2$) is defined to be strictly linear, this is not in general true for all lateral positions y: Because of the geometry of our design, it is the period, not the k-vector, that is a weighted average of that at the $y = \pm W/2$ ends of the device. The next-order phase contribution can be calculated from the design geometry, and we require that the higher-order phase be less than $\pi/2$ for all positions y and all domains along the sample length to reduce resultant higher-order phase on the SH pulse. This requirement imposes the following constraint on the chirp tuning range:

$$(D_a - D_b)^2 < \frac{24\pi^2}{\Lambda_0 L^3}\,. \tag{4}$$

It should be noted that modified design geometries with slightly curved domain walls can eliminate the higher-order phase contribution.

Inequality (4) in turn restricts the maximum fan angle (relative to the crystal axis) to less than $\phi_{\max} = (3\Lambda_0 L/8W^2)^{1/2}$, limiting the fan angle for our devices ($L = 4.7$ cm, $W = 1$ cm, $\Lambda_0 = 18.6$ μm) to less than 4 deg. However, we have found in practice that fabrication proves to be a tighter angular constraint in PPLN when current fabrication techniques are used. Because the domain walls have a preferred orientation along the crystallographic y axis, additional domain spreading results for patterns that have been fabricated with other orientations, requiring the use of correspondingly narrowed poling electrodes to maintain the desired 50% duty cycle. Although fanned domains have been demonstrated for angles as wide as 20 deg,[9] we found experimentally that beyond 2 deg it becomes difficult to maintain the desired duty cycle for QPM gratings with periods near 19 μm.

We performed QPM SHG tunable pulse compression at a FH wavelength of 1.554 μm with a PPLN grating measuring 4.7 cm long and 1 cm wide and a nominal QPM period $\Lambda_0 = 18.6$ μm. The grating length was chosen according to guidelines in Ref. 6 such that the grating bandwidth was roughly three times the $1/e$ spectral width of the pulse. Grating chirps ranged from $D_1 = 0.21$ mm^{-2} (QPM periods from 18.1 to 19.2 μm) to $D_2 = 0.36$ mm^{-2} (QPM periods from 17.8 to 19.7 μm). With a GVM parameter of $\delta\nu = 0.31$ ps/mm, these values imply that the QPM grating is capable of compensating for FH pulse chirps that range from -0.46 to -0.27 ps^2.

Transform-limited pulses of 140-fs (intensity FWHM) duration at a carrier wavelength of 1.554 μm, from a Spectra-Physics OPAL synchronously pumped optical parametric oscillator, are chirped by double-passing of a grating pair pulse stretcher in the Treacy configuration[10] to 8.2-ps ($C_1 = -0.375$ ps^2) FWHM duration. The spectrum and the autocorrelation of the FH pulses are measured after the pulse stretcher. The FH autocorrelation measures 12.7 ps in duration, and the bandwidth is measured to support 140-fs FH pulses and so is capable of generating SH pulses as short at 100 fs at the transform limit for the approximately Gaussian pulse shape. The resultant 1-nJ pulses are then focused into the PPLN crystal, which is housed in a temperature-controlled oven held at 120 °C. The average powers of the FH and the SH beams are measured after the PPLN sample, as are the autocorrelation and the power spectrum of the SH field.

The tuning behavior is shown in Fig. 2. The theoretical curve is calculated to include second- and third-order dispersion ($C_{\text{cubic}} = \mathrm{d}^3\Phi_1/\mathrm{d}\omega^3$ has a value of 1.5×10^{-3} ps^3) for the grating-pair pulse stretcher,[11] showing good agreement between theory and experiment. Our PPLN device is designed with a linearly chirped grating and therefore compensates for only the linear chirp (quadratic phase) on the FH pulse. The minimum measured autocorrelation width is 200 fs, which is 1.4 times the autocorrelation

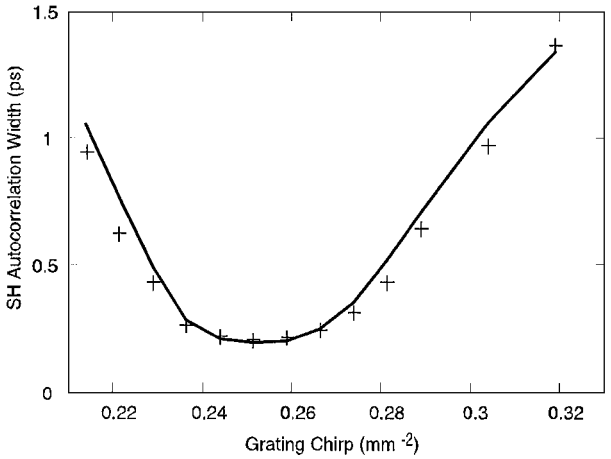

Fig. 2. Tuning behavior of the fanned grating device. The measured autocorrelation width is plotted (crosses) versus grating chirp. A calculated theoretical curve (solid curve) is plotted for comparison.

width of 140 fs for transform-limited pulses. A simple modification of the grating design from the linear chirp given in Eq. (1) to

$$K_g(x) \equiv 2\pi/\Lambda(x) = K_m + 2D_g x + 3Gx^2 \qquad (5)$$

would permit complete compensation for the cubic phase as well, a significant advantage of QPM designs.[4,5] To compensate for the cubic phase (assumed here to be much less than the quadratic phase component), one should choose G such that $G = C_{\text{cubic}}\delta v^3/3{C_1}^3$. Appropriately chosen G_a and G_b coefficients will lead to the construction of a tunable grating design analogous to Eq. (3) for which the linear and the quadratic grating chirps tune together.

The experiment was conducted with confocal focusing ($w_0 = 75\ \mu$m). Power-normalized conversion efficiency (${U_2}/{U_1}^2$, where U_1 and U_2 are the pulse energies of the FH and SH fields, respectively) was observed to be 0.9 %/nJ (pulse energies $U_{\text{FH}} = 0.88$ nJ and $U_{\text{SH}} = 7.58$ pJ). Reference 6 predicts that the conversion efficiency for a chirped QPM PPLN device will be $0.59(\tau_0/\tau_1)\eta_0$, where η_0 (162 %/nJ at a FH wavelength of 1.55 mm) is the efficiency for an unchirped FH pulse and a uniform grating at a length of $2\tau_0/\delta\nu$. Our measured efficiency is 63% of the calculated theoretical value of 1.54 %/nJ.

In conclusion, we have demonstrated QPM SHG pulse compression with tunable dispersion through the use of a fanned grating design. The demonstrated compression ratio of 63 (variable from 50 to 90) with our stretcher and the QPM SHG compressor can be improved with a slight modification of the QPM design to include cubic phase. Straightforward extension of the method to implement general pulse shaping in QPM SHG[6] and in QPM difference-frequency generation[7] devices is possible. Future studies may include other tunable QPM devices, including tunable two-color SHG[12] and tunable compensation of higher-order pulse chirp.

We are grateful for the support of U.S. Air Force Office of Scientific Research grant F49620-99-1-0270 and for the generous donations of lithium niobate wafers by Crystal Technology and of laser equipment by Spectra-Physics. A. M. Schober's e-mail address is schober@stanford.edu.

References

1. M. A. Arbore, O. Marco, and M. M. Fejer, Opt. Lett. **22,** 865 (1997).
2. P. Loza-Alvarez, M. Ebrahimzadeh, W. Sibbet, D. T. Reid, D. Artigas, and M. Missey, J. Opt. Soc. Am. B **18,** 1212 (2001).
3. M. A. Arbore, A. Galvanauskas, D. Harter, M. H. Chou, and M. M. Fejer, Opt. Lett. **22,** 1341 (1997).
4. L. Gallman, G. Steinmeyer, U. Keller, G. Imeshev, M. M. Fejer, and J.-P. Meyn, Opt. Lett. **26,** 614 (2001).
5. K. Green, A. Galvanauskas, K. K. Wong, and D. Harter, in *Nonlinear Optics: Materials, Fundamentals and Applications*, Vol. 46 of OSA Trends in Optics and Photonics Series (Optical Society of America, Washington, D.C., 2000), pp. 113–115.
6. G. Imeshev, M. A. Arbore, M. M. Fejer, A. Galvanauskas, M. Fermann, and D. Harter, J. Opt. Soc. Am. B **17,** 304 (2000).
7. G. Imeshev, M. M. Fejer, A. Galvanuskas, and D. Harter, J. Opt. Soc. Am. B **18,** 534 (2001).
8. P. E. Powers, T. J. Kulp, and S. E. Bisson, Opt. Lett. **23,** 159 (1998).
9. S. Russell, M. Missey, P. Powers, and K. Shepler, in *Conference on Lasers and Electro-Optics (CLEO)*, Vol. 39 of OSA Trends in Optics and Photonics Series (Optical Society of America, Washington, D.C., 2000), pp. 632–633.
10. E. B. Treacy, IEEE J. Quantum Electron. **QE-5,** 454 (1969).
11. J. D. McMullen, Appl. Opt. **18,** 737 (1979).
12. G. Imeshev, M. M. Fejer, A. Galvanauskas, and D. Harter, Opt. Lett. **26,** 268 (2001).